ELSEVIER

Journal of Power Sources 108 (2002) 1–7

JOURNAL OF POWER SOURCES

www.elsevier.com/locate/jpowsour

Electrocatalytic properties of a nickel–tantalum–carbon alloy in an acidic electrolyte

D.R. McIntyre, A. Vossen, J.R. Wilde, G.T. Burstein*

Department of Materials Science and Metallurgy, University of Cambridge, Pembroke Street, Cambridge CB2 3QZ, UK

Received 25 June 2001; received in revised form 3 November 2001; accepted 5 November 2001

Abstract

Amorphous films of mean composition $Ni_{33}Ta_{41}C_{26}$ were prepared by deposition onto carbon paper using dc magnetron sputtering. The material showed low corrosion currents and significant electrocatalytic activity for hydrogen oxidation and oxygen reduction when polarised potentiostatically in 1.5 M H_2SO_4 at 20 and 70 °C. The results are interpreted in terms of the passivity of the tantalum component offering corrosion protection to the nickel electrocatalytic component in the aggressive acidic electrolyte. © 2002 Published by Elsevier Science B.V.

Keywords: Hydrogen oxidation; Oxygen reduction; Acidic electrolytes; Base electrocatalysts; Fuel cells; Passivity; Tantalum carbide

1. Introduction

Fuel cells offer potentially highly efficient, silent, low-pollution electric power generation. To date however, technical and economic barriers have prevented their widespread application to automotive traction and residential power use. Fuel cells with acidic electrolytes are required for use with fuels of commercial purity containing oxides of carbon. One of the key technical factors hampering commercialisation of low-temperature acidic fuel cells is their dependence on the rare platinum-group metals as electrocatalysts, since platinum is both expensive and readily poisoned by carbon monoxide. Research into generation of electrocatalysts made from non-noble materials which can operate efficiently in low-temperature acidic electrolytes is thus a very worthwhile field of inquiry. For anode electrocatalysts, tungsten carbide has been cited as a possibility [1] and combinations of nickel with tungsten carbide [2] and molybdenum with tungsten carbide [3] showed some activity. For the cathode electrocatalysts, various porphyrins have been suggested [4], and some cobalt-based and iron-based electrocatalysts have also been investigated [5,6]. The present paper is a preliminary report into nickel–tantalum based materials.

In order to be considered suitable for fuel cell electrocatalysts, candidate materials made from non-noble elements must be passive towards corrosion in the acidic electrolytes, in contrast to the noble platinum-based systems. Tantalum is well known for its passivity in mineral acids [7]. The passivating oxide film is however, electrically-insulating which makes the surface unsuitable for any form of electrocatalysis [8]. Tantalum carbides, by contrast, are electronically conductive across a considerable range of compositions [9,10]. This paper reports the electrocatalytic properties of a unique combination of nickel, tantalum and carbon prepared by dc magnetron sputtering.

2. Experimental

2.1. Synthesis and examination of the electrocatalyst

The experimental electrocatalytic material was synthesised as a vacuum-sputtered coating laid down directly onto a porous carbon substrate (Toray carbon paper type TGPH-090). The carbon paper, which contains 8% polytetrafluoroethene (PTFE) by weight added as a wet-proofing agent, was in the form of a 25 mm diameter disk, enabling it to be used directly in the electrochemical cell as a test electrode. The coating investigated was composed of nickel, tantalum and carbon, of mean thickness 0.7 μm. This film was deposited by dc planar magnetron sputtering in an ultra-high vacuum chamber using a three-target system, with one target for each component (Ta, Ni and C) [11]. The carbon-paper substrate was rotated under the three different isolated targets at a rate calculated to produce less than a monolayer of each component on each pass, thereby forming a metastable alloy rather than a multilayered structure. A base pressure of 10 pbar was obtained. Sputtering was carried out

* Corresponding author. Tel.: +44-1223-334-361; fax: +44-1223-334-567.
E-mail address: gtb1000@cus.cam.ac.uk (G.T. Burstein).

0378-7753/02/$ – see front matter © 2002 Published by Elsevier Science B.V.
PII: S0378-7753(01)01009-6

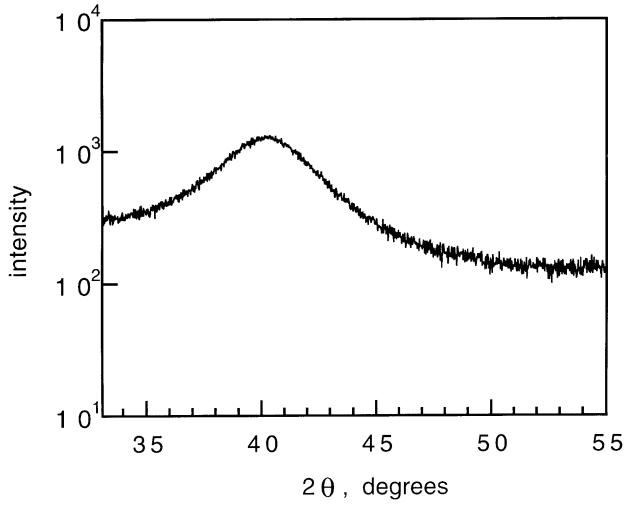

Fig. 1. X-ray diffraction pattern of sputtered $Ni_{33}Ta_{41}C_{26}$.

in argon at a pressure of 6 mbar. The resulting sputtered coating was largely amorphous. X-ray diffraction patterns showed a broad amorphous halo (full width at half maximum intensity, $2\Theta = 4.6^{\circ}$) as shown in Fig. 1. A transmission electron micrograph of the material, presented in Fig. 2, showed that the amorphous phase contained ultra-fine particles of a carbide, presumably tantalum carbide, of diameter ca. 2 nm. The TaC (1 1 1) reflection is missing from Fig. 1 since the carbides form with a strong out-of-plane ⟨1 0 0⟩ texture. The average composition of the coating, as measured by Rutherford backscattering (RBS) analysis [12], was $Ni_{33}Ta_{41}C_{26}$ (atomic composition). Because the alloy is clearly not single phase, but rather a nanocomposite, it is strictly speaking wrong to represent its atomic composition as a single compound, viz. $Ni_{33}Ta_{41}C_{26}$. However, to retain its mean composition in reference, we refer below to the sputtered coating as $Ni_{33}Ta_{41}C_{26}$. Fig. 3 presents an SEM micrograph of the carbon paper surface coated with the 0.7 μm thick $Ni_{33}Ta_{41}C_{26}$ coating.

The catalyst loading of the sputter-coated electrode (i.e. the sputtered carbon, nickel and tantalum layer) was 0.93 mg cm^{-2}. The true surface area of the test electrode was measured by nitrogen adsorption in an automated Gemini 2360 V5 instrument using the Brunauer–Emmett–Teller (BET) technique. The wet-proofed carbon paper alone, with no catalyst loading, gave no measurable surface area by nitrogen adsorption, presumably because of the polytetrafluoroethene content. The nitrogen adsorption data for the sputter-coated electrode showed a true surface area of 22.4 cm^2. Since the projected surface area of the electrode was 4.9 cm^2, the ratio of the true to projected surface area was 4.6.

2.2. Experimental procedure

The electrode was tested for electrocatalytic activity potentiostatically. The electrochemical cell consisted of a PTFE counter electrode chamber containing a platinum foil counter electrode, an electrically heated PTFE electrolyte chamber with a gas-lift electrolyte pump, a Luggin probe for connection to the external reference electrode, the test electrode of 2.4 cm^2 exposed surface area, a current collector of Nb or Au sheet, and a PTFE gas compartment with inlet and outlet connections for feed gas and exhaust. The reference potential was a mercury/mercurous sulphate (MMS) electrode mounted in a side-arm and connected via an electrolyte-filled tube to the Luggin capillary. Its

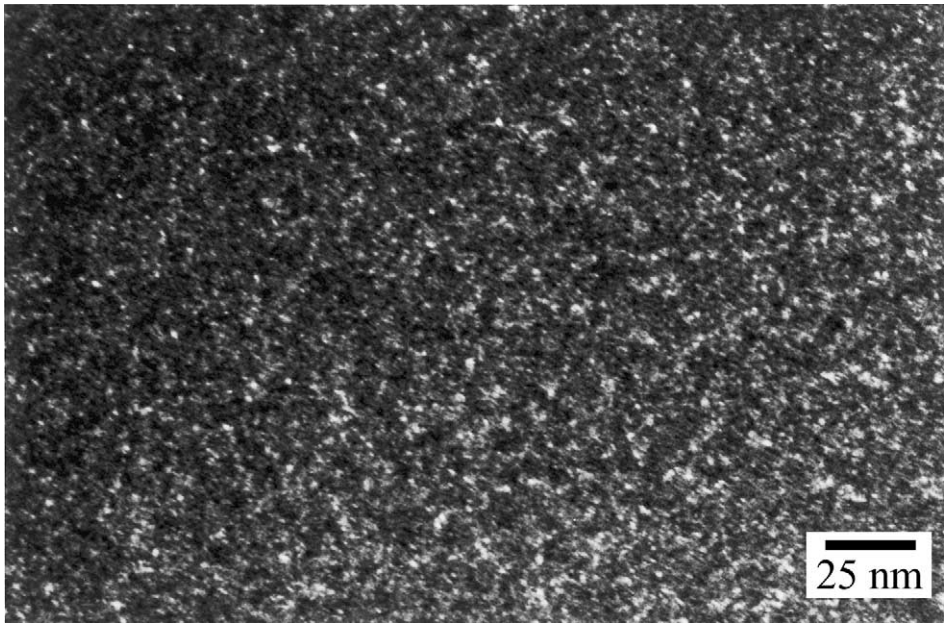

Fig. 2. Transmission electron micrograph of sputtered $Ni_{33}Ta_{41}C_{26}$, showing the presence of ultrafine particles of diameter ca. 2 nm in an amorphous matrix. The particles are probably tantalum carbide.

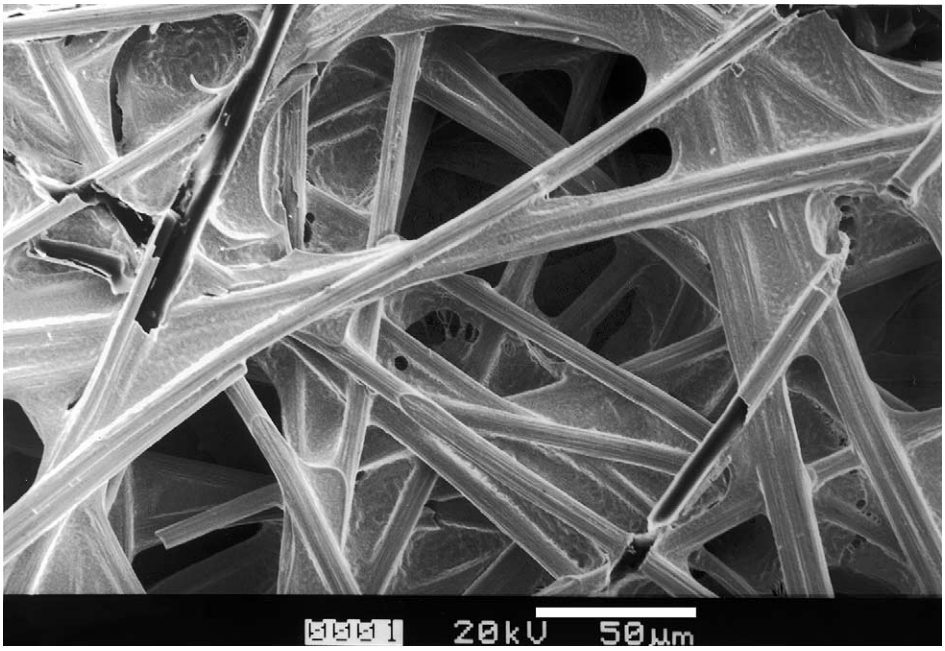

Fig. 3. Micrograph of $Ni_{33}Ta_{41}C_{26}$ of thickness 0.7 μm prepared by sputtering the elements onto carbon paper (Toray TGPH-090).

reference potential, against which the results below are presented, was calibrated and found to be 0.405 V relative to a saturated calomel reference electrode (SCE). The counter electrode was separated from the working electrode compartment by a microporous borosilicate glass frit to prevent gas generated at the counter electrode from reaching the working electrode, whilst at the same time maintaining electrolytic contact through the cell. The electrodes were mounted so as to be cylindrically symmetrical into the internally cylindrical cell. The temperature in the cell was maintained thermostatically using a heating element on an arm of the gas-lift pump and an electronically-read thermistor within the cell. All experiments were carried out at constant temperature.

The test material was subject to three types of electrochemical experiment. Because the electrocatalyst was synthesised from base components, corrosion/passivation tests in the sulphuric acid working electrolyte are vital, and these were performed first in the absence of any fuel. Potentiostatic corrosion tests were followed by examination of the electrocatalytic activity towards the anodic oxidation of hydrogen. Finally, the electrocatalytic activity towards the cathodic reduction of oxygen was also examined.

Potentiostatic corrosion testing was carried out as follows. Initially, the test electrode was placed in the cell with the catalyst side facing the fuel compartment (away from the electrolyte). The cell was assembled and filled with 1.5 M H_2SO_4 made from analytical-grade H_2SO_4 and twice-distilled water. High purity argon was introduced into the gas-lift pump to circulate the electrolyte. Argon was bubbled through the electrolyte continuously for at least an hour before each test, and throughout the course of each test. This was to remove residual oxygen in the electrolyte.

Once the electrolyte had been argon-saturated, a series of potentiostatic transients at incremental intervals of 0.1 V covering the range −0.65 to +0.25 V (MMS) were imposed. These were conducted at 20 and at 70 °C to determine the corrosion current as a function of potential. Each potential step gave a corrosion current recorded as a function of time for 250 s using a digital data acquisition rate of 1 Hz. The final current reading after 250 s was taken to be a quasi-steady state current (Section 3).

The electrode was then examined for electrocatalytic activity towards the anodic oxidation of hydrogen as follows. Once the baseline corrosion current data in the argon-saturated electrolyte had been obtained, another potentiostatic transient was initiated at −0.4 V (MMS). After 50 s, the argon feed to the gas compartment was switched off and hydrogen at ca. 121 kPa absolute pressure was introduced into the fuel chamber. The current–time trace was examined for evidence of a significant rise in anodic current. If such a rise occurred, the hydrogen was switched off and the argon was reintroduced into the fuel chamber, to see if the anodic current declined again. The purpose of this preliminary procedure was to check that it was indeed the hydrogen which was being oxidised. A full series of potentiostatic transients ranging from −0.65 to +0.05 V (MMS) in incremental steps was then recorded with hydrogen flowing through the fuel chamber. At each potential, the current was measured as a function of time for 250 s and recorded. The full test procedure, including both corrosion and hydrogen oxidation analysis, was then repeated with the electrolyte held at a constant temperature of 70 °C.

The material was also tested for electrocatalytic activity towards the cathodic reduction of oxygen. In this case the potentiostatic transients were measured over the potential

range +0.25 to −0.65 V (MMS) through decremental steps of 0.1 V at both 20 and 70 °C, with high purity oxygen flowing through the gas compartment. This maximum applied potential was chosen to be significantly below the oxygen equilibrium potential (0.58 V (MMS) at 25 °C), and the minimum potential limited to be higher than the equilibrium potential for the hydrogen reaction so that no evolution of oxygen or hydrogen could occur. Most of the data described below concerns experiments carried out at 70 °C.

3. Results

Fig. 4 shows a graph of current as a function of time for the $Ni_{33}Ta_{41}C_{26}$ electrode potentiostatically polarised at −0.4 V (MMS) at 20 °C, with the feed gas alternating between argon and hydrogen. The graph shows unambiguously that the material is electrocatalytically active towards the H_2 oxidation reaction: admission of hydrogen causes the current to rise anodically to 65 μA cm^{-2}, and removal of the hydrogen supply causes decay in the anodic current. (Note that the change of gas supply requires some time to equilibrate, ca. 120 s in this case; this is the time required to replace fully one gas by the other within the connecting tubing and the gas compartment.) The residual cathodic current observed prior to hydrogen admission ($t < 50$ s in Fig. 4) must arise from the reduction of a trace of residual dissolved oxygen, despite purging with argon. Irrespective of that however, it shows that at this potential, the rate of anodic oxidation of the electrocatalyst itself must be very small, since it is clearly swamped by the reduction of the residual trace of oxygen.

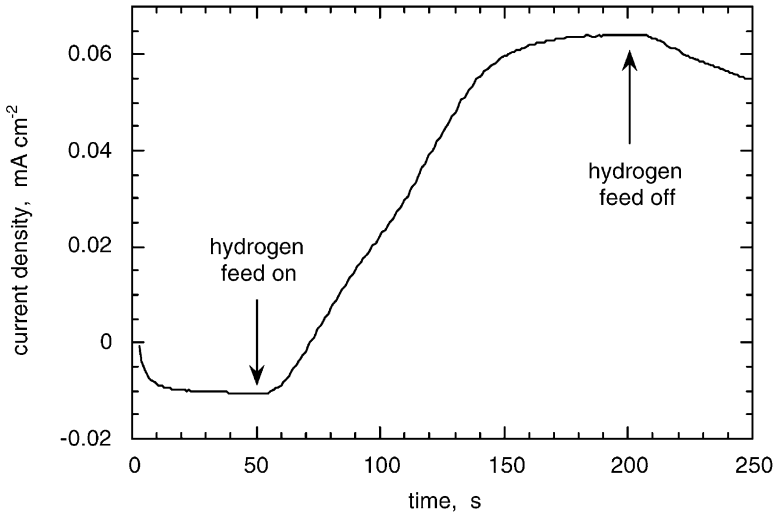

Fig. 4. Current density from $Ni_{33}Ta_{41}C_{26}$ in 1.5 M H_2SO_4 at 70 °C showing the effect of hydrogen as fuel. For the first 50 s, argon was fed over the electrode. Hydrogen was admitted at 50 s and continued until 200 s, after which it was replaced by argon again.

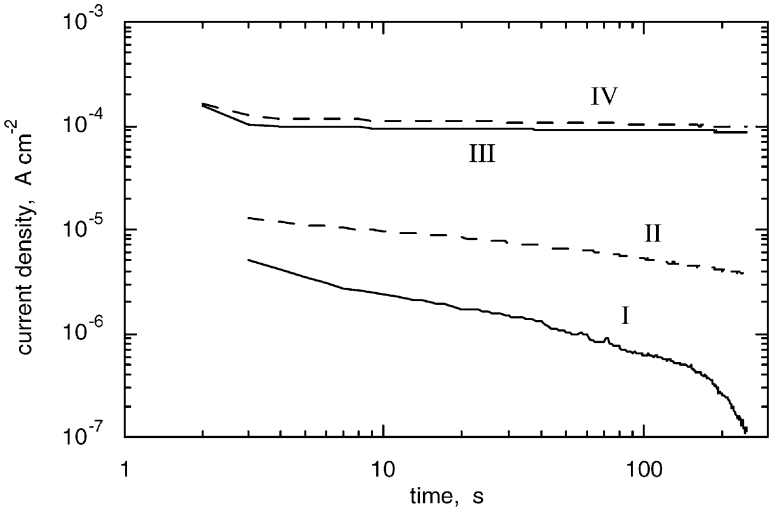

Fig. 5. Anodic current time transients measured on $Ni_{33}Ta_{41}C_{26}$over 250 s in 1.5 M H_2SO_4 at 70 °C showing the effect of hydrogen admission. Argon feed gas at: (I) −0.35 and (II) −0.05 V (MMS). Hydrogen feed gas at: (III) −0.35 and (IV) −0.05 V (MMS).

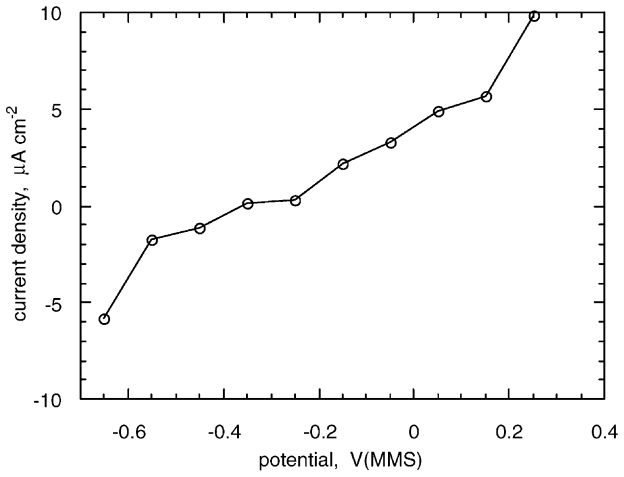

Fig. 6. Polarisation of $Ni_{33}Ta_{41}C_{26}$ in 1.5 M H_2SO_4 at 70 °C under argon atmosphere. Each data point shows the non-fuelled reaction rate of the material measured 250 s after the start of polarisation.

The low corrosion rate of the catalyst in hot sulphuric acid is shown in Fig. 5, where a set of current/time transients measured at an electrolyte temperature of 70 °C is plotted. The corrosion rates are low for all the potentials shown, and they decline continuously with time throughout the recording period. The material thus passivates continuously. The low corrosion rate is confirmed by the corrosion data measured after 250 s, shown in Fig. 6 as a function of potential. This material passivates against corrosion at all the applied potentials in hot sulphuric acid, and the process of passivation is still not complete after 250 s. The highest corrosion rate observed was at the maximum applied potential; even here, the corrosion rate was only 10 μA cm^{-2} after 250 s, and still declining.

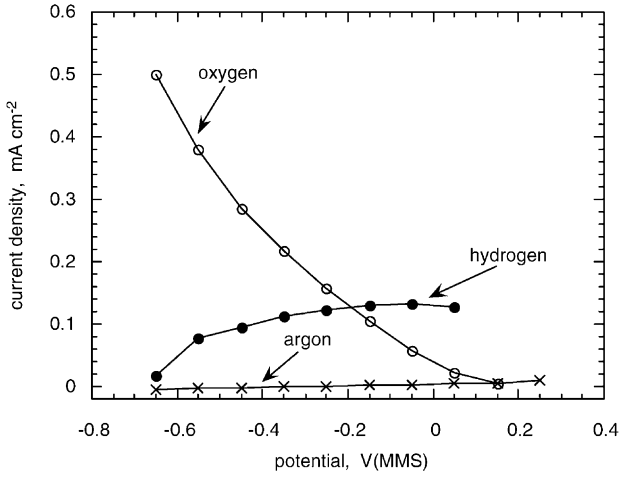

Fig. 7. Reaction rates describing anodic oxidation of hydrogen (black points) and cathodic reduction of oxygen (white points) gases fed over $Ni_{33}Ta_{41}C_{26}$ electrocatalyst in 1.5 M H_2SO_4 at 70 °C. The background current density of the electrocatalyst over argon is also shown (crosses). The data represent the rates measured 250 s after commencement of the potentiostatic transient.

The rates of reaction with the two reactive gases, hydrogen and oxygen, are shown in Fig. 7 for experiments at 70 °C. Both the anodic oxidation of hydrogen and the cathodic reduction of oxygen are electrocatalysed on this material. The hydrogen oxidation rate reaches an apparent limiting current density of ca. 130 μA cm^{-2}. The oxygen reduction current density rises continuously with decrease in potential, and does not reach a limiting value.

4. Discussion

In order to function successfully as an electrocatalyst made of base materials in such a strongly acidic electrolyte, three criteria must be met. First, the material must be very passive towards corrosion; such passivity in aqueous solution is engendered normally by the growth of an oxide film [7,8,13]. Second, the passivated surface must be electron conducting to allow the electrode reaction to occur through the surface film. Third, the surface must be electrocatalytically active towards the desired reaction. We note that pure tantalum passivates by the growth of an electronically insulating oxide film [7,8], and thus could not itself function as an electrocatalyst. To make it electrocatalytic, is must be made to conduct electrons in its passive state. The new material is clearly both passive against corrosion at all potentials in hot sulphuric acid, as well as electrocatalytic to both hydrogen oxidation and to oxygen reduction. Bearing in mind that this electrocatalyst has low specific surface area, the results described show significant electrocatalytic activity and very low corrosion rates.

The data above describe the fact that the fabricated coating is highly passive in 1.5 M H_2SO_4 at 70 °C. The passivating current density decays continuously with time of polarisation, and the material can be expected to be still more passive after much longer periods of time. Since the true surface area of the material is 4.6 cm^2/cm^2, an observed current density of 10 μA cm^{-2} (the maximum observed corrosion current density observed at 0.25 V (MMS)) is equivalent to a true value of 2.2 μA cm^{-2}. The fact that this continues to decline further with time, demonstrates clearly the high degree of passivity of this material in the hot acidic electrolyte. The passive current density described above has not in fact yet reached a steady state, even after 250 s of polarisation, and the true passive current density must be even lower. Moreover, no active loop in the polarisation curve (Fig. 6) could be found. The passivating component is without doubt tantalum, whose passivity is brought about by a film of Ta_2O_5 [13]; this oxide is stable in passive acidic solutions and the passivity of Ta is well documented [7,13].

As well as being very passive in strongly acidic electrolyte, the electrode functions as an electrocatalyst for both the anodic oxidation of hydrogen and the cathodic reduction of oxygen. Since these gas reactions must take place at the solid/electrolyte interface, they must occur on the passivated

surface. The passivating oxide on pure tantalum is however an electron insulator, as is evident from the fact that tantalum metal can be anodised to high voltage to produce a thicker oxide [8,14]. One must therefore deduce that the oxide is rendered electron conducting, by the presence of either the carbon component or the nickel component. At these potentials, nickel is thermodynamically stable only in its oxidised form [13], and any nickel present in the surface must be trapped within the oxide matrix. A similar notion was proposed earlier to describe the observed electrocatalytic activity of tungsten-based materials which had also involved co-synthesis with nickel [2,15,16]. If the carbon component provides the required electron conduction in the oxide, then it is likely to remain unoxidised within the surface, since in acidic electrolytes, oxidised carbon would probably be gaseous (CO or CO_2) and thus removed from the surface. Note that the anodic fuel current density reaches a near plateau value after 250 s (Fig. 5), and does not carry on decaying continuously as does the corrosion current.

The electrocatalytic nature of the surface is provided by the nickel component. This proposal is reinforced by the fact that we have made and tested electrodes constructed directly from polycrystalline tantalum carbide alone, in the absence of any nickel. Pure polycrystalline tantalum carbide electrodes were found to be passive in 1.5 M H_2SO_4 at 70 °C; however, we have been unable to detect significant electrocatalytic activity, anodic or cathodic, from the nickel-free carbide. We therefore believe that the surface of the new material reported above, sputter-formed $Ni_{33}Ta_{41}C_{26}$, contains all the original components from the sputtered layer, and these persist under polarisation in sulphuric acid. Nickel is probably in oxidised form trapped in the passivated tantalum oxide/carbide matrix.

The nature of the catalysis is curious. Normally for non-valve metals, as for example occurs on platinum, the oxygen reduction reaction requires significantly greater overpotentials than the hydrogen oxidation reaction [17]. The hydrogen oxidation reaction on $Ni_{33}Ta_{41}C_{26}$ reaches an apparent limiting current density; this cannot be due to mass transport limitation, since the oxygen reduction reaction on the same electrode does not reach such a limiting current density (Fig. 6). If mass transport of the gas were to become rate-limiting, then the limiting rate of anodic reaction would be expected to be reflected also in the cathodic regime, after allowing for the factor of two difference in stoichiometric number of the two gas reactions; this is contrary to observation.

One possible conclusion could be that the anodic reaction rate may become limited by electron conduction through the surface film, with some rectification of the electron current through the surface film, so that the cathodic reaction was not thus affected. However, we tested this catalyst in separate experiments using equimolar ferricyanide/ferrocyanide mixed electrolyte, and found that the cathodic reduction of $Fe(CN)_6^{3-}$ occurred at an approximately equal rate to the anodic oxidation of $Fe(CN)_6^{4-}$ at equal overpotentials. This implies that there is no rectification, at least at modest overpotentials. Another possibility would be that the rate limiting step switches to a non-electrochemical reaction step, such as the dissociation of H_2 to adsorbed atomic H on the surface. This limiting current density for hydrogen oxidation is a clear drawback of the present anode; its origins are not yet clear, and the mechanism is being explored further.

However, it is worthwile to point out that this material maintains a high degree of passivity against corrosion, even at high potentials, where other electrocatalysts made from base materials may lose their passivity. This makes the oxygen reduction reaction a viable process for this material, and this electrocatalysis from Fig. 7 is plain. Other electrocatalysts made from base materials, such as tungsten carbide, are transpassively corroded at higher potentials, and could not survive acidic electrolytes for use as an oxygen cathode. For example, our experiments with tungsten carbide based electrodes show transpassive corrosion commencing at ca. 0.5 V (SCE) (equivalent to −0.15 V (MMS)) [2,15], rendering them immediately unsuitable as cathodes.

In line with other base electrocatalysts, this Ni/Ta/C material does not show the activity (anodic or cathodic) achieved by platinum electrocatalysts, or even approaching that. Hydrogen/oxygen fuel cells using platinum anodes and cathodes, and running at 75–80 °C are capable of over 1 A cm^{-2} (of projected electrode area) at 0.5 V cell voltage, using membrane electrolytes (see e.g. [17,18]). It should nevertheless be mentioned that the electrodes made for the work presented above were of low specific surface area. (The ratio of the true to projected surface areas was 4.6.). High catalytic activity for Pt-based catalysts depends, at least in part, on generating a very high surface area electrode. As an example, high current densities, in excess of 1 A cm^{-2}, were achieved on Pt-based electrodes which were loaded to 4 mg cm^{-2} using electrocatalysts of specific surface are 21–63 $m^2\ g^{-1}$ [18]; these data imply the ratio of the true to the projected areas was between 840 and 2500. We are as yet unable to achieve high surface areas by the magnetron sputtering method.

5. Conclusions

1. A vacuum-sputtered Ni–Ta–C alloy of mean composition $Ni_{33}Ta_{41}C_{26}$, functions as an electrocatalyst both for the anodic oxidation of hydrogen and for the cathodic reduction of oxygen in 1.5 M H_2SO_4 at temperatures up to 70 °C.
2. The electrocatalyst is highly passive against corrosion in 1.5 M sulphuric acid at temperatures up to 70 °C across a wide range of electrode potential, thereby giving very low corrosion rates.
3. Electrocatalytic activity occurs on the passivated surface of the material. Passivity towards corrosion and activity towards the required electrochemical reaction can be common properties of the same surface.

4. The as-sputtered electrocatalytic material consists of a dispersion of ultra-fine tantalum carbide particles, of size ca. 2 nm, immersed in an amorphous matrix of Ni–Ta–C.

Acknowledgements

We are grateful to the Ernest Oppenheimer Fund for financial support of AV. Measurement of surface areas by the BET method was carried out by Dr. K. Balakrisnan, to whom we are grateful.

References

[1] H. Binder, W.H. Kuhn, W. Lindner, G. Sandstede, US Patent 3,708,342 (1973).
[2] C.J. Barnett, G.T. Burstein, A.R.J. Kucernak, K.R. Williams, Electrochim. Acta 42 (1997) 2381.
[3] G. Kawamura, H. Okamoto, A. Ishikawa, T. Kudo, J. Electrochem. Soc. 134 (1987) 1653.
[4] G.Q. Sun, J.T. Wang, R.F. Savinell, J. Appl. Electrochem. 28 (1998) 1087.
[5] G. Lalande, D. Guay, J.P. Dodelet, S.A. Majetich, M.E. McHenry, Chem. Mater. 9 (1997) 784.
[6] H. Wang, R. Côté, G. Faubert, D. Guay, J.P. Dodelet, J. Phys. Chem. B 103 (1999) 2042.
[7] J. Bentley, in: L.L. Shreir, R.A. Jarman, G.T. Burstein (Eds.), Corrosion, 3rd Edition, Vol. 1, Butterworths, London, 1995, p. 5.62.
[8] L. Young, Anodic Oxide Films, Academic Press, London 1961, p. 4.
[9] E.K. Storms, The Refractory Carbides. Academic Press, New York, 1967, p. 108.
[10] L.E. Toth, Transition Metal Carbides and Nitrides, Academic Press, New York, 1971, p. 187.
[11] R.E. Somekh, Z.H. Barber, J. Phys. E: Sci. Instrum. 21 (1998) 1029.
[12] C. Jeynes, N.P. Barradas, J.R. Wilde, A.L. Greer, Nucl. Instrum. Meth. B 161 (2000) 287.
[13] G.T. Burstein, in: L.L. Shreir, R.A. Jarman, G.T. Burstein (Eds.), Corrosion, 3rd Edition, Butterworths, London, 1994, p. 1.118.
[14] T.P. Hoar, in: J.O'M. Bockris, B.E. Conway (Eds.), Modern Aspects of Electrochemistry No. 2, Butterworths, London, 1959, p. 262.
[15] G.T. Burstein, C.J. Barnett, A.R.J. Kucernak, K.R. Williams, Catal. Today 38 (1997) 425.
[16] G.T. Burstein, C.J. Barnett, Materials World, 1998, p. 412.
[17] G.J.K. Acres, J.C. Frost, G.A. Hards, R.J. Potter, T.R. Ralph, D. Thompsett, G.T. Burstein, G.J. Hutchings, Catal. Today 38 (1997) 393.
[18] P. Gouérec, M.C. Denis, D. Guay, J.P. Dodelet, R. Schulz, J. Electrochem. Soc. 147 (2000) 3989.